

7.1: Quality Control of WSR-88D Data

V Lakshmanan¹, Kurt Hondl², Gregory Stumpf¹, Travis Smith^{1*}

Abstract

We describe a real-time algorithm for removing non-precipitating echoes from WSR-88D reflectivity data using vertical profiles of reflectivity, Doppler velocity and Spectrum Width. Various attributes, described in this paper, were computed from the radar moments. A few volume scans of radar data were chosen and used to train a feed-forward neural network trained in a supervised manner using resilient-propagation and adaptive weight decay. The trained network was tested on other, independent data cases. The performance of the algorithm was compared to existing methods of performing automated quality control on radar reflectivity data using these independent test cases. We find that the neural-net outperforms the other techniques handily. We also explore the limits on how general the neural network is and make suggestions for quality control in general situations.

1. Introduction

From the point of view of automated applications operating on weather data, echoes in radar reflectivity may be contaminated. These applications require that echoes in the radar reflectivity moment correspond, broadly, to “weather”. By removing ground clutter contamination, estimates of rainfall from the radar data using the National Weather Service (NWS) Weather Surveillance Radar-Doppler 1998 (WSR-88D) can be improved (Fulton et al. 1998; Kessinger et al. 2003). A large number of false positives for the Mesocyclone Detection Algorithm (Stumpf et al. 1995) are caused in regions of clear-air return (McGrath et al. 2002). Poor segmentation and forecasting are achieved by a hierarchical motion estimation technique in regions of ground clutter (Lakshmanan et al. 2003; Lakshmanan 2001). Hence, a completely automated algorithm that can remove regions of ground clutter, anomalous propagation and clear-air returns from the radar reflectivity field would be very useful in improving the performance of other automated weather algorithms.

The problem of examining the radar moments for automated removal of non-precipitating echoes has been

the focus of some research by Steiner and Smith (2002) and Kessinger et al. (2003). The Radar Echo Classifier (REC) described in (Kessinger et al. 2003) has been implemented into the operational Open Radar Product Generator (ORPG). It incorporates the ideas introduced in (Steiner and Smith 2002) and hence, provides a good baseline for comparison. In this paper, the development of a neural network (NN) to do the same task is described. We compare the neural network's performance on independent cases with the Radar Echo Classifier (REC).

2. The Neural Networks

The final set of features used in the network for which results are reported were: for the lowest scan of velocity, spectrum width and the second lowest scan of reflectivity: local mean, local variance, difference between the data value and the mean, for the lowest scan of reflectivity: local mean, local variance, difference between the data value and the local mean, REC Texture (Kessinger et al. 2003), homogeneity, SPIN (Steiner

¹V Lakshmanan, Gregory Stumpf and Travis Smith are with the Cooperative Institute of Mesoscale Meteorological Studies (CIMMS), University of Oklahoma. ²Kurt Hondl is with the National Severe Storms Laboratory, Norman, OK

and Smith 2002), number of inflections at a 2dBZ threshold, SIGN (Kessinger et al. 2003), echo size. Features related to the vertical profile of reflectivity were the maximum value, weighted average, difference between data values at the two lowest scans, echo top height at a 5dBZ thresholds.

To decorrelate the data value from the mean and median, the difference between the data value and the local mean was used. The weighted average of the reflectivity values is computed over all the elevations where the weight of each data point is given by the height of that pixel above the radar. This takes into account the entire vertical profile instead of just the first two elevations. The homogeneity of the reflectivity field is defined as:

$$hom_{xy} = \frac{\sum_{i \in N_{xy}} \frac{1}{1 + (\frac{I_{xy} - I_i}{I_{xy}})^2}}{card(N_{xy}) - 1} \quad (1)$$

where N_{xy} is the set of valid pixels (I_i) in the neighborhood, N_{xy} , of the pixel at (x, y) in the image, I_{xy} is the pixel value and $card(N_{xy})$ is the number of such neighbors. Echo-size is defined as the fraction of neighbors whose values are within 10dBZ of this pixel's reflectivity value. An inflection point is defined similar to the SPIN (Steiner and Smith 2002) except that the inflection is defined not in a polar neighborhood, but along the entire radial until that point.

We used two separate neural networks – one in regions where Doppler Velocity and Spectrum Width are available, and another where they aren't. All the neural network inputs were scaled such that each feature in the training data exhibited a zero mean and a unit variance when the mean and variance are computed across all patterns.

a. Network Architecture

We used a resilient backpropagation neural network (RPROP) described in Riedmiller and Braun (1993). The RPROP network was trained using supervised batch learning in a multi-layer perceptron (MLP) network. There was one hidden layer. Every input unit was connected to every hidden unit, and every hidden unit to the output unit. In addition, there was a short-circuit connection from the input units directly to the output unit, to capture any linear relationships. Every hidden node

had a “tanh” activation function, chosen because of its signed range. The output unit had a sigmoidal activation function so that the outputs of the networks could be interpreted as posterior probabilities (Bishop 1995). Each non-input node had, associated with it, a bias value which was also part of the training.

The error function that was minimized was a weighted sum of the cross-entropy (which Bishop (1995) suggests is the best measure of error in binary classification problems) and the squared sum of all the weights in the network. The weight decay term improves generalization (Krogh and Hertz 1992). The relative weight, λ , of the two measures is computed within a Bayesian framework (MacKay 1992; Bishop 1995).

The with-velocity network had 22 inputs, 5 hidden nodes and one output while the reflectivity-only network had 16 inputs, 4 hidden nodes and one output.

A validation set ensures a network's generalization, typically through the use of early stopping methods (Bishop 1995). In the neural network literature, a validation set is usually utilized to select the architecture of the neural network. We did not use a separate validation set, mainly because we did not have enough training data in order to do so. Because we lacked a validation set, we did not consider any alternate network topologies. A different network topology may outperform our neural network. Weight decay, rewarding smaller weights, is an alternative way to ensure generalization (Krogh and Hertz 1992; Bishop 1995).

We did use an independent testing set, as described in Section 3.. An extended form of this study, could involve training with the current training set, validating with the current testing set, and then testing on a newly gathered and truthed set of cases. Such a study could make use of early stopping as well.

Just eight volumes of WSR-88D data were selected to encompass different scenarios – strong convection, stratiform rain, ice-coating, low-topped cells, etc. A human interpreter examined these volume scans and drew polygons using the WDSS-II display (Hondl 2002) to select “bad” echo regions. An automated procedure used these human-generated polygons to classify every pixel into the two categories (precipitating and non-precipitating).

Radar Echo Classifier							
Number	nulls	false-alarms	miss	hit	POD	FAR	CSI
1	48554	2573	579	512	0.47	0.83	0.14
2	1187	161	0	0	nan	1	0
3	13440	23	24648	17927	0.42	0	0.42
4	46124	20474	1033	1126	0.52	0.95	0.05
5	10420	14	20798	13828	0.40	0	0.40
6	29731	629	4965	7562	0.60	0.08	0.57
total	149456	23874	52023	40955	0.44	0.37	0.35

Neural Network							
Number	nulls	false-alarms	miss	hit	POD	FAR	CSI
1	50346	781	271	820	0.75	0.49	0.44
2	419	929	0	0	nan	1	0
3	13363	100	5489	37086	0.87	0	0.87
4	25517	41081	7	2152	1	0.95	0.05
5	10259	175	3828	30798	0.89	0	0.88
6	14697	15663	76	12451	0.99	0.56	0.44
total	114601	58729	9671	83307	0.90	0.41	0.55

Table 1: Skill scores when classifying using the Radar Echo Classifier and when using the Neural Network.

3. Results and Conclusions

For testing, a diverse set of volume scans of weather data were chosen and bad echoes marked on these volume scans by a human observer. The volume scans are listed below:

1. KAMA Apr 18, 2002 07:19:10 to 07:23:49 – Significant AP.
2. KFSX Jan 10, 2003 16:12:09 to 16:20:20 – Terrain-induced ground clutter.
3. KTLX May 14, 2003 13:41:08 to 13:45:45 – Strong convection with sharp gradients.
4. KTLX May 19, 2003 08:57:52 to 09:06:02 – AP and spatially smooth clear-air return.
5. KINX May 20, 2003 10:25:52 to 10:30:31 – Strong convection close to the radar.
6. KTLX May 20, 2003 16:39:14 to 16:44:30 – Clear-air return at several elevations.

The volume scans were processed using the trained neural network and using the Radar Echo Classifier (Kessinger et al. 2003). Comparisons were made on a pixel-by-pixel basis of all pixels for which at least one of the elevations had a reflectivity value greater than zero

The neural network identifies regions of precipitation with high skill. It is able to identify bad echoes (AP/GC) when they are similar to cases that it has seen before, but is not able to deduce unfamiliar situations (terrain-

dBZ. Nulls refer to pixels which are not weather-related, and are correctly classified. Hits refer to pixels which are weather-related and are correctly classified. Misses refer to weather-related echoes that are missed, while false-alarms refer to non-weather echoes that are incorrectly classified.

The confusion matrices for each of the volume scans are shown in Table 1 for the two algorithms being compared. The first row of Figure shows a case of significant AP/GC while the third row shows a significant precipitation event. Looking at these images, it is possible to put the quantitative measures (cases 1 and 3) in context. We see that a lot of good data is misclassified by the Radar Echo Classifier. At the same time, the neural network makes its mistakes on lower reflectivity values, but gets higher reflectivity values (whether AP/GC or good data) correct more often. This is a consequence of the cost factors used in the network error equation.

Terrain-induced ground-clutter (Jan. 10, 2003 from KFSX, shown in the second row of Figure) was not part of the training regimen of the neural network, and does pose problems. In mountain regions, terrain heights, or the height of the echo above terrain, could be part of the inputs to the network, instead of, as currently, simply the height above the radar. The network would also have to use texture statistics from the second tilt of the radar, and use vertical differences for the lowest three tilts.

induced GC, vertically continuous clear-air return, chaff, etc.) Even with these limitations, however, the neural network greatly outperforms existing automated techniques. At locations where one or more of these bad-echo forma-

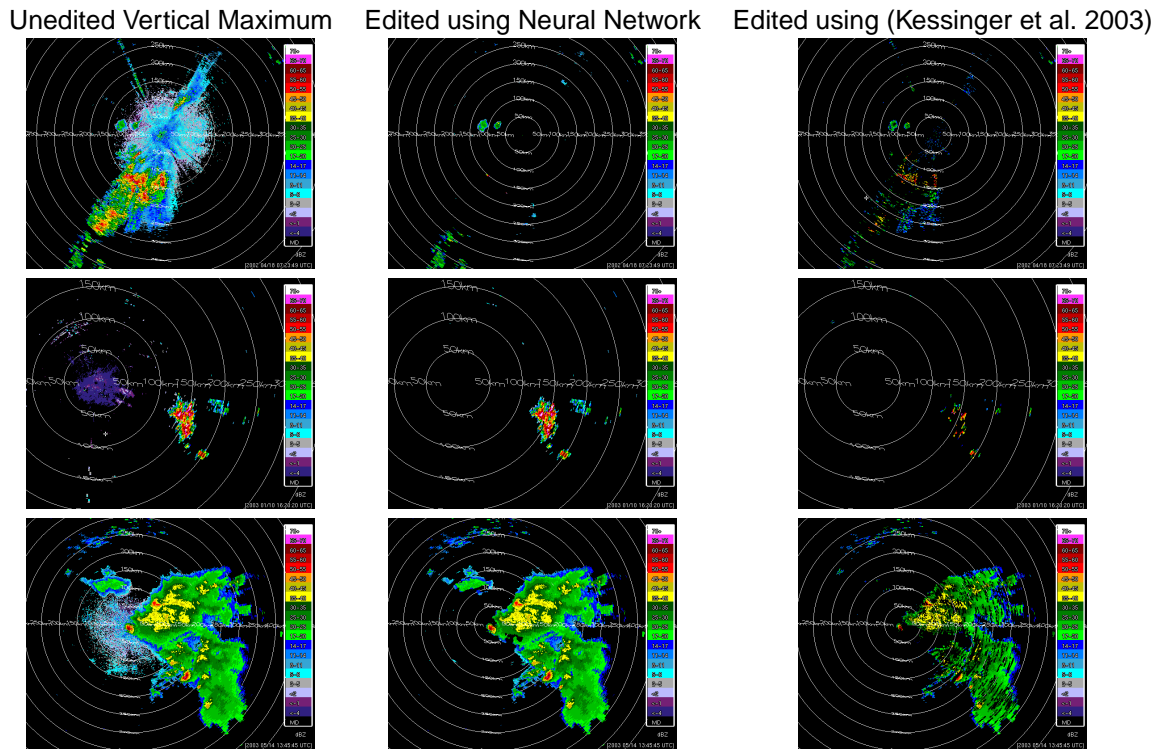


Figure 1: Selected testing cases: KAMA 4/18/2002, KFSX 1/10/2003 and KTLX 5/14/2003. Performance on a data case with significant AP/GC is shown in the first row. The second row illustrates that the Neural Network performs poorly on cases from the Mountain West, where it was not trained, while the third row shows a typical spring precipitation event from the Great Plains.

tions is frequent, the neural network should be trained with those. The network, if trained judiciously, shows high skill in “remembering” and removing bad-echo patterns that it has been trained on.

Acknowledgement Funding for this research was provided under NOAA-OU Cooperative Agreement NA17RJ227, FAA Phased Array Research MOU, and the National Science Foundation Grants 9982299 and 0205628.

References

- Bishop, C., 1995: *Neural Networks for Pattern Recognition*. Oxford.
- Fulton, R., D. Breidenback, D. Miller, and T. O'Bannon, 1998: The WSR-88D rainfall algorithm. *Weather and Forecasting*, **13**, 377–395.
- Hondl, K.: 2002, Current and planned activities for the warning decision support system-integrated information (WDSS-II). *21st Conference on Severe Local Storms*, Amer. Meteor. Soc., San Antonio, TX.
- Kessinger, C., S. Ellis, and J. Van Andel: 2003, The radar echo classifier: A fuzzy logic algorithm for the WSR-88D. *19th IIPS Conference*, Amer. Meteor. Soc., Long Beach, CA.
- Krogh, A. and J. Hertz: 1992, A simple weight decay can improve generalization. *Advances In Neural Information Processing Systems*, S. H. Moody, J. and R. Lippman, eds., Morgan Kaufmann, volume 4, 950–957.
- Lakshmanan, V., 2001: *A Hierarchical, Multiscale Texture Segmentation Algorithm for Real-World Scenes*. Ph.D. thesis, U. Oklahoma, Norman, OK.
- Lakshmanan, V.: 2003, Real-time quality control of reflectivity using satellite infrared channel and surface observations. *Royal Met. Soc. Conf. 2003*, Norwich.
- Lakshmanan, V., R. Rabin, and V. DeBrunner, 2003: Multiscale storm identification and forecast. *J. Atmospheric Research*, ??
- MacKay, D. J. C.: 1992, A practical Bayesian framework for backprop networks. *Advances in Neural Information Processing Systems 4*, J. E. Moody, S. J. Hanson, and R. P. Lippmann, eds., 839–846.
- McGrath, K., T. Jones, and J. Snow: 2002, Increasing the usefulness of a mesocyclone climatology. *21st Conference on Severe Local Storms*, Amer. Meteor. Soc., San Antonio, TX.
- Moller, M., 1993: A scaled conjugate gradient algorithm for fast supervised learning. *Neural Networks*, **6**, 525–533.
- Riedmiller, M. and H. Braun: 1993, A direct adaptive method for faster backpropagation learning: The RPROP algorithm. *Proc. IEEE Conf. on Neural Networks*.
- Steiner, M. and J. Smith: 2002: Use of three-dimensional reflectivity structure for automated detection and removal of non-precipitating echoes in radar data. *J. Atmos. Ocea. Tech.*, 673–686.
- Stumpf, G., C. Marzban, and E. Rasmussen: 1995, The new NSSL mesocyclone detection algorithm: a paradigm shift in the understanding of storm-scale circulation detection. *27th Conference on Radar Meteorology*.
- Verikas, A., K. Malmqvist, A. Lipnickas, M. Bacauskiene, and A. Gelzinis, 1999: Soft combination of neural classifiers. *Pattern Recognition Letters*, **20**, 429–444.